Proceedings of Insert Conference Abbreviation:
Insert Conference Name
Insert Conference Date and Location

Put Paper Number Here

PERFORMANCE MEASUREMENT OF THE SECOND STAGE OF A TRANSONIC TURBINE

A.Seyr, G. Kulhanek, F. Neumayer, E. Rossi[1)] and W. Sanz

Institute for Thermal Turbomachinery and Machine Dynamics
Graz University of Technology, Austria
[1)]Nuovo Pignone, Firenze, Italy

ABSTRACT

In November 1999 the turbine test facility at the Institute for Thermal Turbomachinery and Machine Dynamics was completed. This test stand is a cold flow transonic test turbine facility, which is a unique combination of a 2.3 MW axial test turbine and a directly-coupled compressor that generates about the half of the compressed air needed to drive the turbine. To cover the losses, additional air is provided by an electrically-driven compressor station. A 600 kW suction blower driven by a helicopter gas turbine is used to decrease the exhaust pressure, thus increasing the expansion ratio up to 4.5 (see Erhard and Gehrer “Design and Construction of a Transonic Test-Turbine Facility”, ASME Paper 2000-GT-480).

Since then, flow measurements with two different transonic turbine stages have been carried out.

This paper will focus on the description of the measurement system, data analysis and the newest test results that have been obtained on a turbine stage developed by Nuovo Pignone. This stage has been configured to be representative of advanced designs for medium/small land based gas turbines and is characterized by high pressure ratios and strongly transonic effects. The characteristic feature of this stage is the convergent- divergent flow channel. Basic data of this turbine stage to obtain flow similarity are: 2.2 MW shaft power at 11500 rpm, pressure ratio 4.5, mass flow 22 kg/s. The paper will contain appropriately plotted results of dimensionless stage characteristic curves over a broad range of operation points.

NOMENCLATURE

a	Speed of Sound
c	Velocity
D	Diameter
d/D	Diameter ratio
h	Specific enthalpy
$\dot{m}$	Mass flow
N	Shaft speed
P	Power
T	Temperature

Greek

h	Efficiency
k	Isentropic exponent
m	Dynamic viscosity
r	Density

Subscripts

DP	Theoretical design point
e	effective
is	isentropic
u	circumferential
01	Total inlet conditions

INTRODUCTION

In common one can observe two tendencies in gas turbine development. The first is the claim for higher efficiencies and the second is to decrease the costs per kW shaft power. High efficiencies can be mainly obtained by increasing the turbine inlet temperature. Cost reduction can be reached by having a high mass flow rate at a given shaft speed, less stages and therefore a high pressure drop over each single stage. Note that the transition from a relative Mach number of 0.9 to 1.3 results in an increase of mass flow rate of a factor 2.4, Bölcs and Suter, 1986.

Within the scope of the project S6801-TEC, “Efficiency improvement by flow optimization”, of the Austrian Science Foundation and the BRITE EURAM project DITTUS, “Development of Industrial Transonic Turbine Stages”, a new transonic test turbine rig was constructed.

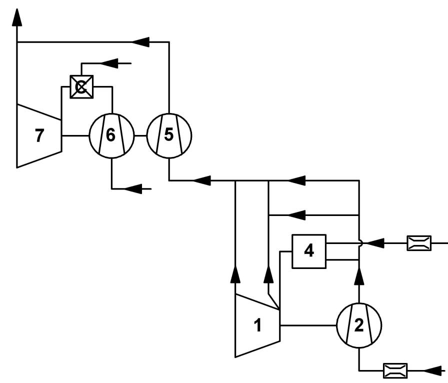

Figure 1. The test turbine plant

This test facility offers the possibility to do research not only on one turbine stage with a given geometry but to investigate various turbine stages in cooperation with different manufacturers. This test rig shown in figure 1 consists of six main parts where (1) is the turbine stage under investigation, (2) the GHH brake compressor, (3) the compressor station sited in the basement of the building, (4) the mixing chamber in which the two air flows, the one from the brake compressor and the one from the compressor station, are fed and (5) the suction blower driven by a former helicopter gas turbine (6), (7). A more detailed description of the plant will be given in Neumayer et al., 2001.

The first turbine stage under investigation was the so called TTM-stage, shown in figure 2, which was designed and constructed by members of the Institute for Thermal Turbomachinery and Machine Dynamics, Graz University of Technology. This stage is thought of a research turbine stage for conventional and optical measurements. With this stage the commissioning of the whole plant was performed during winter 1999/2000, see Erhard and Gehrer, 2000.

The second turbine stage under investigation was a scaled down model of a high pressure ratio transonic stage designed by Nuovo Pignone which has been built and installed in the test rig. During the summer, intensive measurement work was done resulting in a complete turbine map of this stage. The meridional section of the model is shown in figure 3. This stage has guide vanes in front of the stator to simulate the first stage. Throughout this paper this stage will be called NP2 stage.

Both turbine stages have the convergent-divergent meridional section in common. The shape of the channel resembles a Laval nozzle and has the function to place the smallest sectional area at a clearly defined point. There the flow reaches Mach 1 and then the mass flow is determined by the smallest sectional area, the upstream total pressure and the upstream total temperature only. The main difference concerning the meridional section is that the TTM stage has a completely cylindrical inner contour to make optical measurement easier and that the meridional section of the TTM stage has its smallest height within the stator at the position where Mach 1 shall occur.

EXPERIMENTAL FACILITY

The instrumentation of the test turbine consists of two main parts. The first part, the plant control and surveillance system, is the basic instrumentation which is necessary to operate the facility and to collect operation data. It is possible to get a complete description of the plant behavior with these data. In addition it is also possible to describe fundamental characteristics of the turbine stage with these data. The second part of the instrumentation serves to investigate the characteristics of the turbine stage in a more detailed manner. Both parts of the instrumentation system shall be described in detail in the following chapters.

Control and surveillance scheme

The instrumentation for control and surveillance of the plant is the basic measurement equipment which is a fixed part of the test rig. It stays on the machine even if there are different turbine stages under investigation. The measured quantities are the mass flow from the compressor station, the mass flow from the brake compressor, turbine inlet and outlet conditions, shaft speed and torque, bearing and oil temperature and the oil mass flow.

The air mass flow from the compressor station is measured with a standard DIN Venturi nozzle. Total and difference pressures are measured with Druck PMP 4000 pressure scanners with an accuracy of 0.04 % best straight line (BSL). The temperature of the air flow is measured with a three wire Pt 100 sensor. The same set up is applied to the mass flow measurement of the brake compressor, with the Venturi nozzle placed at the beginning of the pipe line close after the inlet filter as the only difference. Due to the fact that the mass flow from the compressor station and from the brake compressor are nearly the same, both Venturi nozzles can be calibrated by means of a single transonic Venturi nozzle especially designed to meet the upper part of the operation range.

The total pressures and temperatures in the mixing chamber and in

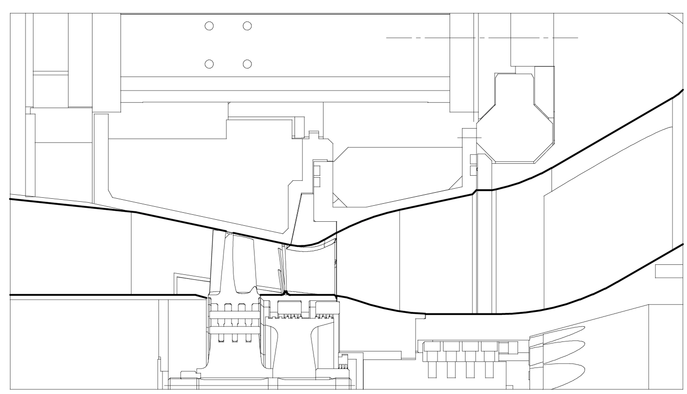

Figure 2. Meridional section of the TTM stage

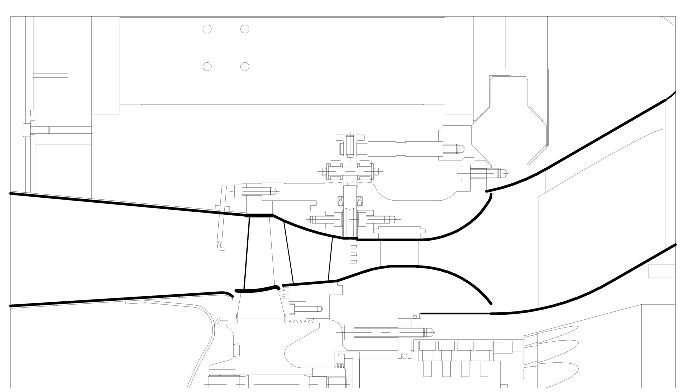

Figure 3. Meridional section of the NP2 stage

the exhaust line are measured with PMP 4000 pressure scanners and Pt 100 sensors.

The measurement of shaft speed, torque, vibration and bearing temperatures is done with a BentlyNevada 3300 system; the oil mass flows through each of the four bearings are measured with turbine flow meters.

Stage Measurement Set Up

Instrumentation for the determination of stage characteristics has to meet not only high demands on accuracy and repeatability but require higher numbers of channels, too. Therefore the measurement system is made up by five multi channel pressure transducers PSI 9016 with a total amount of 80 channels and an accuracy of 0.05 % and four National Instruments Field Point FP-TC-120 eight-channel thermocouple input modules and one FP-RTD-122 resistance thermometer input module.

The National Instruments Field Point FP-TC-120 thermocouple input modules purchased at the beginning of the project suffer from low accuracy. The limiting factor is the built-in thermistor which measures the reference temperature of the junctions. To overcome this problem the FP-TC-120 modules are used as A/D voltage converters only whereas the cold junctions are placed in isolated isothermal copper blocks. The temperatures of the blocks are measured by means of Pt 100 sensors with the FP-RTD-122 resistance thermometer input module. After calibration of the whole measurement chain the repeatability was better than 0.1 °C. Calibration was performed by means of a calibration oven and a standardized Pt 100 sensor.

It is this remaining uncertainty in temperature measurement which represents the main uncertainty in efficiency measurements. Depending on the pressure ratio and therefore the temperature drop over the stage the accuracy of efficiency measurements is between η (%)$\pm$0.09 (%) at a pressure ratio of 4 and $\pm$0.19% at a pressure ratio of 2.

Whereas the test runs carried out with the TTM test turbine stage primarily had the purpose to show the behavior of the whole plant and the possibility to drive at different operation points, the NP2 stage was completely instrumented in three planes.

In plane A in front of the stator there were three total pressure rakes and three total temperature rakes in circumferential direction with five positions in radial direction each and static pressure taps in the outer wall of the casing. Static pressure was measured in plane B between the rotor and the stator in the outer wall, too. In plane C which is located after the rotor there were a total temperature rake with ten equally spaced measurement points in radial direction and another ten thermocouples equally spaced in circumferential direction at midspan.

Total pressure, static pressure and flow angle were measured with a 2D cobra probe which could be traversed in radial direction by means of a stepper motor. Static pressure was measured at the outer wall, too. In addition the static pressure was measured at the end of the diffuser at the inner and the outer wall.

Data Acquisition Network

The network layout of the plant is shown in figure 4. Voltage and current signals from single-channel transducers are converted with National Instruments Field Point modules placed as near as possible to the sensors to keep cable lengths short. The digitalized data is sent via a RS 485 network to the measurement PC where visualization and data storage takes place. Shaft and bearing data coming from the BentlyNevada System is sent via the RS 232 net to the same PC. The PSI pressure scanners have their own network. They share a common hub and are directly connected to the institute's network. Because of the high data rate a second PC is used to store the data coming from the PSI pressure scanners. The two PCs are connected with each other to share data necessary for online visualization during the test run.

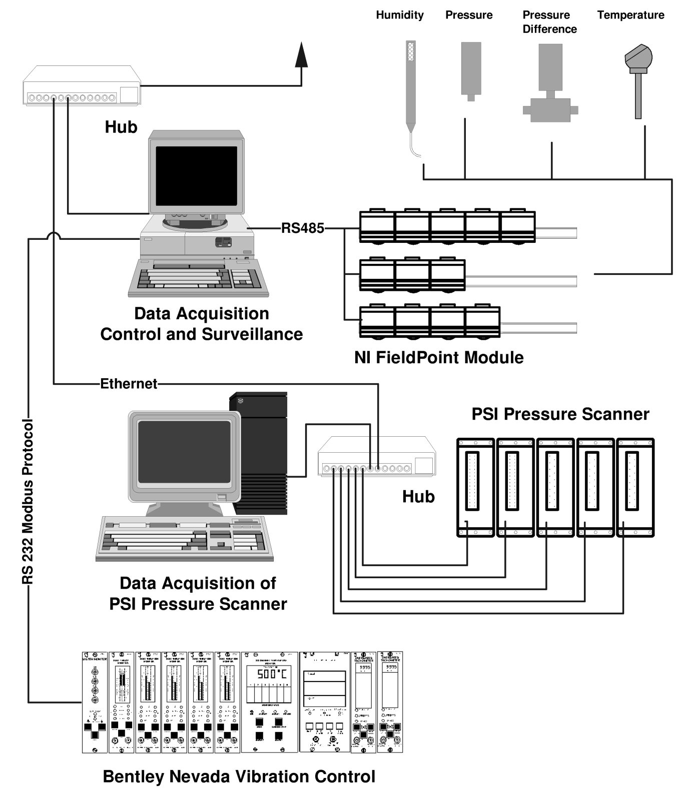

Figure 4. Data acquisition network

Measurement Software

Simultaneously with the building of the test rig the data acquisition program was developed. On one hand this software is capable to provide the operator of the plant with all necessary data during the test run, on the other hand it manages completely the data storage procedure, the analysis of these data and the administration of all sensors within the system. Administration means that the properties of each single sensor are stored in a database together with a name which is characteristic for a single sensor. So adjusting the measurement system to different tasks simply means to add, edit, or delete a data set within the database. Measuring a quantity now is to send an inquiry with the sensors name to the database which will deal with device and channel numbers, the method of transforming a signal into a SI unit, and what kind of calibration curve has to be applied to the concerning sensor. The whole procedure is shown in figure 5. A copy of the database used during the test run is stored together with the data. The data acquisition program is completely written in G, the graphical program language of LabView from National Instruments.

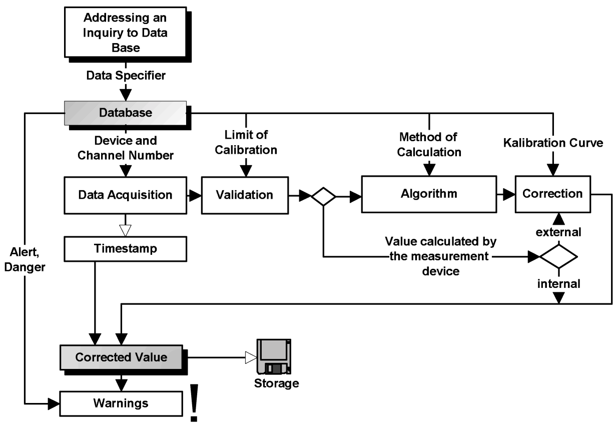

Figure 5. Data acquisition procedure

TURBINE MAPPING PROCEDURE

As previously mentioned, the design of the test rig allows to investigate different stages at different conditions. In order to compare the performance of different stages with each other, all measured quantities are written in non dimensional form using the Π-product method consequently. The Π-products result from a dimensional analysis of a set of performance variables, see Wright, 1999 and Volponi, 1999. This set of performance variables as well as the relation between measured quantities and Π-products can be found in table 1. It should be noted that one can derive almost all different kinds of turbine maps which exist throughout literature in the Π-product form by simply combining different Π-products as can be seen in table 2.

An additional advantage of the use of Π-products is that one can obtain different but comparable descriptions from one and the same map which helps to avoid errors due to smoothing techniques applied to scattered data. Especially in the area near the design point, where efficiency lines or speed lines, depending upon the method, are very close to each other, it is often difficult to decide which shape the curve has to have and wether the data is physically meaningful or not. Changing to another method of presentation often makes it easier to get a better understanding of the data.

The commonly used plot of efficiency versus pressure ratio with

Table 1. Π-Products

$\Delta h_{0,is} = f_1(N, D, \dot{m}, T_0, \rho_0, \mu, \kappa, \frac{d}{D})$ $P = f_2(N, D, \dot{m}, T_0, \rho_0, \mu, \kappa, \frac{d}{D})$ $\eta = f_3(N, D, \dot{m}, T_0, \rho_0, \mu, \kappa, \frac{d}{D})$		$\Pi_1 = \rho^a N^b D^c \dot{m}$ $\Pi_2 = \rho^a N^b D^c P$ $\Pi_3 = \rho^a N^b D^c \Delta h_{0,is}$ $\Pi_4 = \rho^a N^b D^c a_{01}$ $\Pi_5 = \rho^a N^b D^c \mu$	
$\Pi_1 = \frac{\dot{m}}{\left(\rho_{01} N D^3\right)}$	mass flow coefficient	$\Pi_4 = \frac{ND}{a_{01}}$	Mach Number
$\Pi_2 = \frac{P}{\left(\rho_{01} N^3 D^5\right)}$	power coefficient	$\Pi_5 = \frac{\rho_{01} N D^2}{\mu}$	Reynolds Number
$\Pi_3 = \frac{\Delta h_{0,is}}{\left(N^2 D^2\right)}$	work coefficient		

the corrected speed as parameter lines for example can easily be extracted from a turbine map written in Π-product form.

In this case the efficiency versus pressure ratio plot gets the form efficiency versus $\Pi_3\Pi_4^2$ with Π_4 as parameter lines. The diagram type efficiency versus velocity ratio which is described in Kurzke, 1996 can also be derived from an appropriate turbine map having the form efficiency versus $1/\Pi_3\Pi_4$with Π_4 as parameter lines. If these plots are extracted from a correctly smoothed turbine map, the shape of the parameter lines in the new plot must be smooth and meaningful, too.

Examples of both plots will be given for the NP2 stage later in this paper.

The Π_2/Π_1 vs $\Pi_1\Pi_4^2$ Turbine Map

This kind of turbine map according to method 4 in table 2 is useful when the characteristic of a complete gas generator, a free running combination of a compressor and a turbine without external power output, shall be described. Because the test turbine set up is very similar to such a configuration this map format became a practical tool for the planning of different test runs and shall be described in brief in this chapter.

This map shows iso-efficiency lines and iso-lines of the circumferential Mach number as parameters. On the y-axis the value Π_2/Π_1 is a measure for the enthalpy drop, whereas the value $\Pi_1\Pi_4^2$ on the x-axis indicates the flow through the turbine. If there are transonic conditions

Table 2. Methods of turbine mapping with corresponding Π-products

				Method	A Non Dimensional Characteristics				B Dimensional Characteristics			
					Flow	Enthalpy Drop	Speed	Efficiency	Flow	Enthalpy Drop	Speed	Efficiency
$\Delta h_{0,is} = f_1(N, D, \dot{m}, T_0, \rho_0, \mu, \kappa, \frac{d}{D})$ $P = f_2(N, D, \dot{m}, T_0, \rho_0, \mu, \kappa, \frac{d}{D})$ $\eta = f_3(N, D, \dot{m}, T_0, \rho_0, \mu, \kappa, \frac{d}{D})$		$\Pi_1 = \rho^a N^b D^c \dot{m}$ $\Pi_2 = \rho^a N^b D^c P$ $\Pi_3 = \rho^a N^b D^c \Delta h_{0,is}$ $\Pi_4 = \rho^a N^b D^c a_{01}$ $\Pi_5 = \rho^a N^b D^c \mu$		1	$\varphi = \frac{c_{ax,0}}{u} \triangleq \Pi_1$	$\psi = \frac{2\Delta h_{0,is}}{u^2} \triangleq \Pi_3\Pi_4$	$M_u = \frac{u}{a_{00}} \triangleq \Pi_4$	η	$\frac{\dot{V}_0}{N}$	$\frac{H_{00}}{N^2}$	$\frac{N}{\sqrt{T_{00}}}$	η
$\Pi_1 = \frac{\dot{m}}{\left(\rho_{01} N D^3\right)}$	mass flow coefficient	$\Pi_4 = \frac{ND}{a_{01}}$	Mach Number	2	$\frac{c_{ax,0}}{a_{00}} \triangleq \frac{\Pi_1}{\Pi_4}$	$\frac{c_{00}}{a_{00}} \triangleq \frac{\sqrt{\Pi_3}}{\Pi_4}$	$M_u = \frac{u}{a_{00}} \triangleq \Pi_4$	η	$\frac{\dot{V}_0}{\sqrt{T_{00}}}$	$\frac{H_{00}}{T_{00}}$	$\frac{N}{\sqrt{T_{00}}}$	η
$\Pi_2 = \frac{P}{\left(\rho_{01} N^3 D^5\right)}$	power coefficient	$\Pi_5 = \frac{\rho_{01} N D^2}{\mu}$	Reynolds Number	3	$\frac{c_{ax,0}}{c_{00}} \triangleq \frac{\Pi_1}{\sqrt{\Pi_3}}$	$\frac{c_{00}}{a_{00}} \triangleq \frac{\sqrt{\Pi_3}}{\Pi_4}$	$\frac{u}{c_{00}} \triangleq \frac{1}{\sqrt{\Pi_3}}$	η	$\frac{\dot{V}_E}{\sqrt{H_{ad}}}$	$\frac{H_{00}}{T_{00}}$	$\frac{N}{\sqrt{H_{00}}}$	η
$\Pi_3 = \frac{\Delta h_{0,is}}{\left(N^2 D^2\right)}$	work coefficient			4	$\varphi M_u^{\ 2} \triangleq \Pi_1\Pi_4^{\ 2}$	$\psi_e = \frac{\Delta h_e}{u^2} \triangleq \frac{\Pi_2}{\Pi_1}$	$M_u = \frac{u}{a_{00}} \triangleq \Pi_4$	η	$\frac{\dot{V}_0}{\sqrt{T_{00}}} \cdot \frac{N}{\sqrt{T_{00}}}$	$\frac{H_e}{N^2}$	$\frac{N}{\sqrt{T_{00}}}$	η

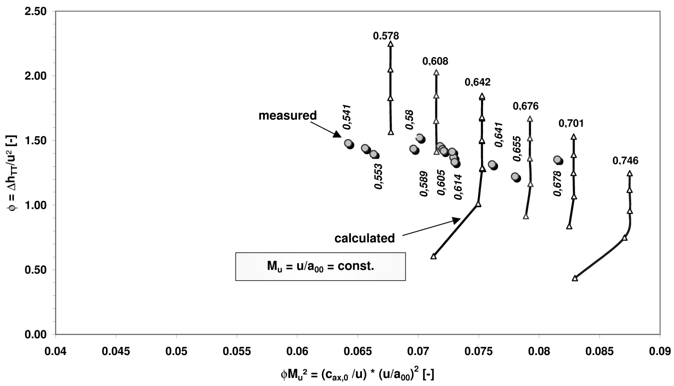

Figure 6. Turbine map of the TTM stage according to method 4

this value changes its meaning. $\Pi_1\Pi_4^2$ can be written as:

$$\left(\frac{\dot{m}}{\rho_{01}ND^3}\frac{ND}{a_{01}}\right)\frac{ND}{a_{01}}$$

In theory the part in parentheses will be constant if there are transonic conditions and the Mach number is one in the narrowest area which normally takes place somewhere within the stator. In this case the remaining second part of the equation which is equivalent to the corrected speed $NT^{-1/2}$ is the circumferential Mach number. This is the reason why the parameter lines are vertical parallel to the y-axis under ideal conditions. This behavior can be seen in figure 6. There the results of several Navier Stokes calculations with a quasi 3D model of the TTM stage at different operation points are shown together with measured data, see Erhard, 2000.

TEST RESULTS

The following test results were derived from a great number of test runs carried out during summer 2000. In contrast to the test runs of the TTM stage, whose results are shown above, the use of the suction blower made it possible to run the test rig at various load conditions. This made it possible to gain complete turbine maps.

Results from Probe Traversing

Figures 7, 8 and 9 show comparison between measured and computational flow traverses at bucket exit.

The computational results were obtained with the TRAFMS97B code. The model is a two stages steady 3D model with constant mass flow. There was no cooling or leakage flow considered. At the inlet total pressure, total temperature and flow angles were specified, at the exit the static pressure is specified. The turbulence model used in this calculation is a conventional Baldwin-Lomax model.

The comparison of total pressure shows good agreement also in tip and root region where local effects are present. The comparison of total temperature and flow angle shows agreement with respect to general shape of the curve, while some offset can be noted which is attributed to unsteady effects present in the experiment and not directly considered in

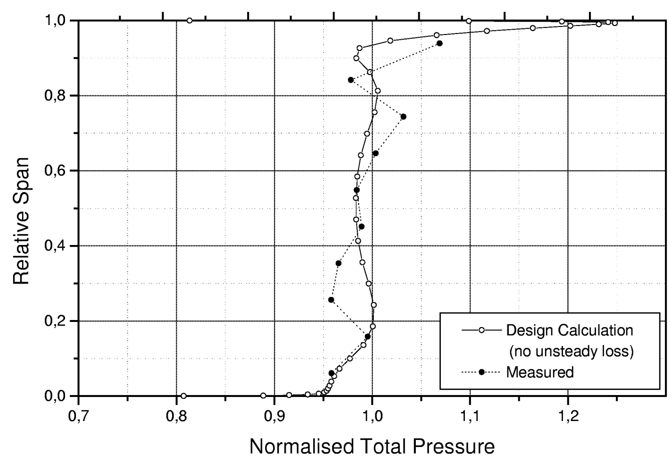

Figure 8. Radial total pressure distribution at stage exit

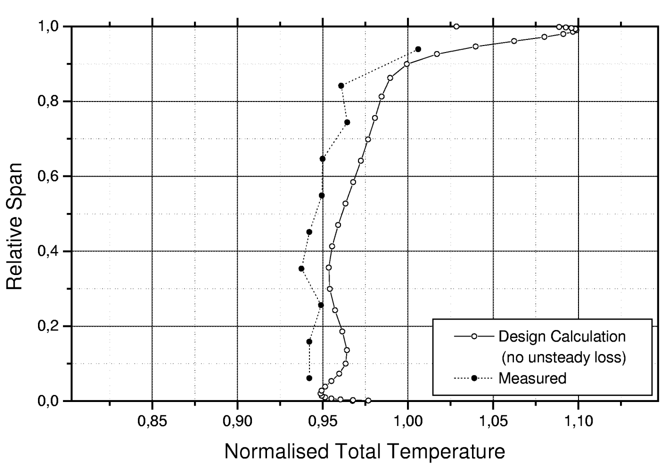

Figure 7. Radial temperature distribution at stage exit

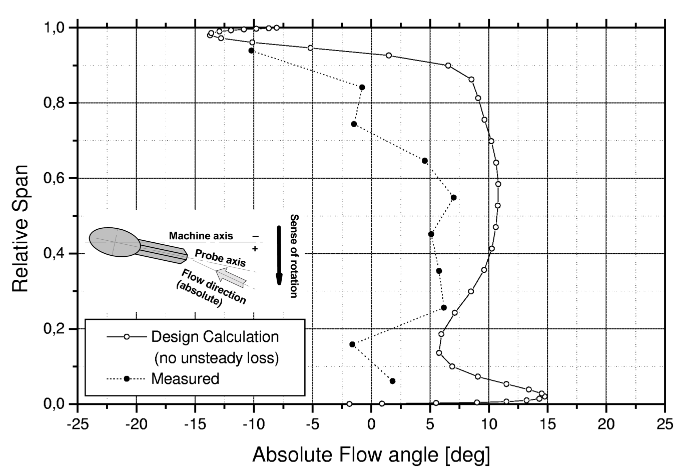

Figure 9. Absolute flow angle at stage exit

the calculations.

Figure 7 shows the radial temperature distribution in the exit plane C behind the rotor measured with ten equally-spaced thermocouples of type J mounted radially on a rake. The average circumferential temperature was measured by means of another ten thermocouples which were equally spaced in circumferential direction in the midspan of plane C.

The turbine is fed by two different air flows, the one from the compressor station and the one from the brake compressor, which have not the same temperature when they enter the mixing chamber. There are some operation points where the temperature difference is higher than 100 °C. The performance of mixing chamber is insufficient when the temperature difference reaches this high value. The result is a non-uniform temperature profile in circumferential direction at the turbine inlet and outlet. In some areas the temperature profile differ ±4% from the average circumferential temperature.

To overcome this error the midspan temperature measured with the radially mounted thermocouple rake was compared to the average circumferential temperature. The difference between this two temperatures was then used to make a temperature offset correction of the whole radially mounted thermocouple rake.

In figures 8–9 the total pressure distribution and the absolute flow angle over the span are shown. These results were obtained from traversing a calibrated cobra probe radially. Flow angle accuracy is

$$\pm(0{,}05° \text{ (Cobra probe intrinsic error)} + 0.5° \text{ (typical alignment error)})$$

Accuracy in total pressure measurement by means of the cobra probe 0.25% of the dynamic pressure. In our test the total accuracy, probe error and scanner error, is about 40 Pa.

These data were used to calculate the mass-averaged quantities which are necessary for efficiency determination.

Turbine Maps

Figure 10 shows the dimensionless corrected mass flow versus pressure ratio. It can be clearly seen that the corrected mass flow reaches an almost constant value which is independent from pressure ratio as long as the operation point lies in the transonic region. This simple relation $\Pi_1\Pi_4 = const$ is a useful characteristic for a numeric simulation of the plant behavior.

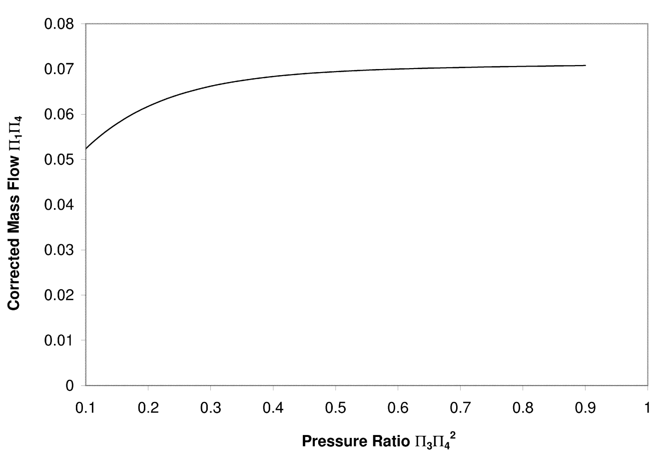

Figure 10. Corrected mass flow vs. pressure ratio using Π-products

The relation between the turbine map according to method 4 and a presentation of efficiency versus pressure ratio is shown in figure 11 and 12 together with measured data points. In these figures data points of several test runs are plotted exceptionally without regard to thermal stability within the system which is the reason why the data points are heavily scattered. This is done to show how the presented method of getting turbine maps can handle even heavily scattered data. The point of intersection P_3 between the iso-lines of efficiency η and corrected speed Π_4 must be somewhere within the dotted lines, figure 11. Having only this plot it is difficult to estimate the point of intersection accurately. But if the power coefficient Π_2 is defined as

$$\Pi_2 = \frac{P}{(\rho_{01}N^3D^5)} = \frac{\dot{m}(h_{01} - h_{03})}{(\rho_{01}N^3D^5)}$$

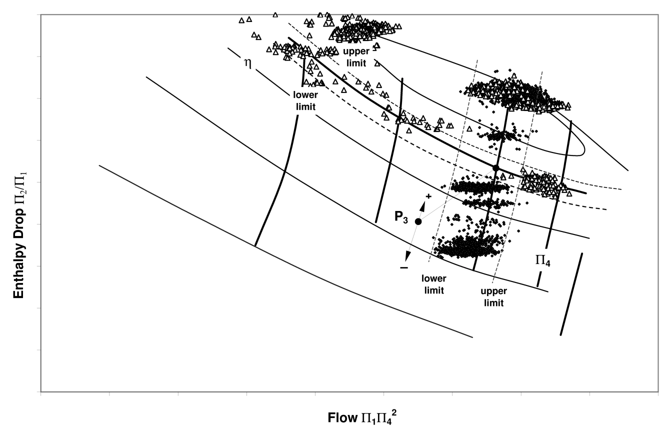

Figure 11. Turbine map according to method 4 with scattered data

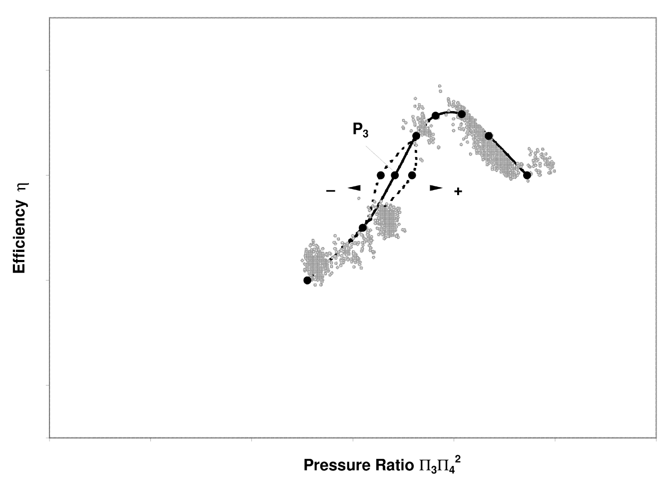

Figure 12. Efficiency vs. pressure ratio with an interpolation curve derived from the turbine map

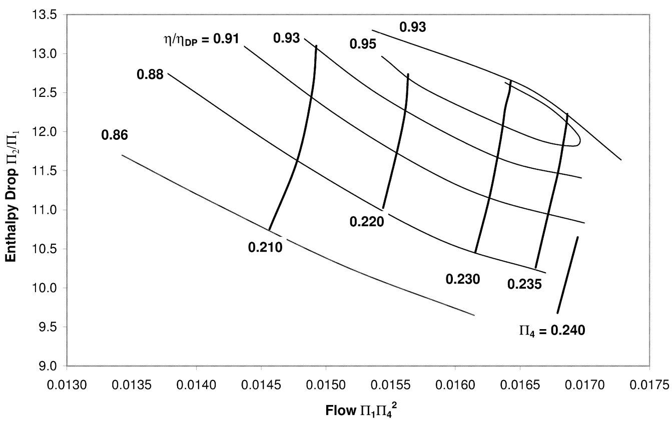

Figure 13. Turbine map of the NP2 stage according to method 4

one can obtain the work coefficient Π_3 from the relation

$$\eta = \eta_{TT} = \frac{\Pi_2}{\Pi_1 \Pi_3}$$

where η_{TT} is the total to total efficiency obtained from the interpolated iso-lines of efficiency in the turbine map in figure 11.

If now the iso-line of corrected speed Π_4 is drawn in the efficiency versus pressure ratio plot, figure 12, together with measured data there is a good control wether the shape of the interpolated curve agrees with the measured data and parameter Π_3 which does not appear directly in a turbine map according to method 4. The double-sided arrow shows then in which direction the interpolated curve has to be adjusted to obtain smooth lines.

The complete turbine map of the NP2 stage with iso-lines of efficiency and corrected speed is shown in figure 13. Figure 14 and figure 15 show the plot of efficiency versus pressure ratio and efficiency versus velocity ratio, respectively. The latter two plots were derived both from the smoothed turbine map and from measured data points. Fitting curves were then choosen in a way that data points were connected by smoothing curves in all three plots simultaneously.

The turbine map in figure 13 shows a good agreement with the ones published in Hausenblas, 1962. Below the maximum point there is a very soft increase in efficiency whereas the iso-lines are very close to each other above the maximum, indicating a fast efficiency decrease with higher enthalpy drop. Iso-lines of corrected speed have an almost vertical shape.In figure 14 iso-lines of corrected speed are shown as parameter lines derived from lines both to the left and to the right of the point of maximum efficiency in figure 13. Because of the shape of the iso-lines of efficiency obtained from the turbine map, these lines may intersect each other.

In figure 15 the velocity ratio written in Π product form is an equivalent expression to:

$$\frac{N/(\sqrt{T})}{(2\Delta h_{is})/T}$$

CONCLUSIONS

The experimental facility and a detailed description of the measurement system used for performance measurements of transonic gas turbine stages at the Institute for Thermal Turbomachinery and Machine Dynamics, Graz, Austria, were presented together with appropriately plotted dimensionless characteristic curves of a scaled model of an industrial gas turbine stage. Efficiency measurements were performed during summer 2000. The advantage of the use of turbine maps in the Π-format for the direct comparability of different maps was shown. In addition it was pointed out that errors resulting from the smoothing of scattered data can easily be avoided if there is the possibility to derive one map from another directly.

Comparison between computed and measured flow characteristics show encouraging agreement.

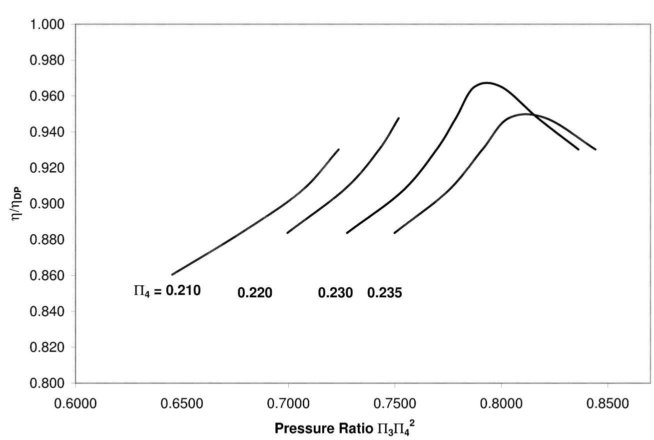

Figure 14. Efficiency vs. pressure ratio using Π-products

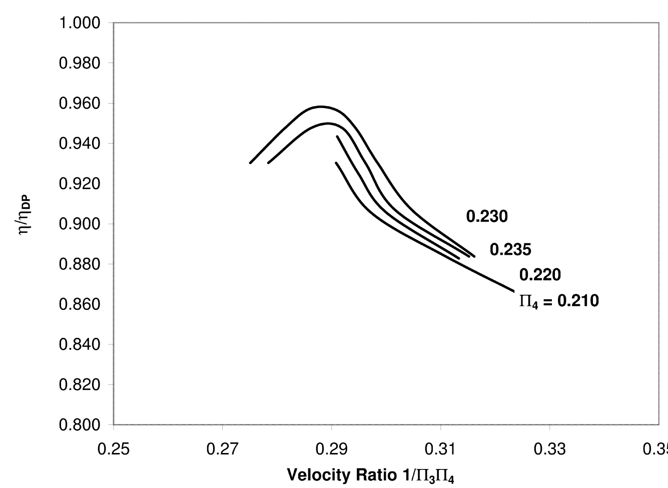

Figure 15. Efficiency vs. velocity ratio using Π-products

ACKNOWLEDGEMENT

The authors gratefully acknowledge the support of the Austrian Science Foundation (FWF) for supporting this work (Project S6801 “Efficiency improvement by flow optimization) as well as the support of the European Commission (Project DITTUS “Development of Industrial Transonic Turbine Stages”)

REFERENCES

Bölcs, A., Suter, P. 1986, “Transsonische Turbomaschinen” G. Braun 1986 ISBN 3-7650-2036-2

Erhard, J. 2000, “Design, Construction and Commissioning of a Transonic Test-Turbine Facility”, Ph.D. Thesis, Graz University of Technology, 2000

Erhard, J., Gehrer, A. 2000, “Design and Construction of a Transonic Test-Turbine Facility”, ASME Paper 2000-GT-480

Hausenblas, H. 1962, “Vorausberechnung des Teillastverhaltens von Gasturbinen”, Springer Verlag 1962, Library of Congress Catalog Card Number: 62-17099

Kurzke, J. 1996, “How to get Component Maps for Aircraft Gas Turbine Performance Calculations”, ASME Paper 96-GT-164

Neumayer, F., Kulhanek, G., Pirker, H.-P., Jericha, H., Sanz, W. 2001, “Operational Behavior of a Complex Transonic Test Turbine Facility”, Paper submitted to ASME TurboExpo 2001

Volponi, A. J. 1999, “Gas Turbine Parameter Corrections”, Journal of Engineering for Gas Turbines and Power, Oct. 1999, Vol. 121 p. 617

Wright, T. 1999, “Fluid Machinery Performance, Analysis and Design”, CRC Press 1999 ISBN 0-8493-2015-1